Pergamon

Chaos, Solitons & Fractals Vol. 9, No. 8, pp. 1373–1390, 1998

Printed in Great Britain
0960–0779/98 $19.00+0.00

PII: S0960-0779(98)00070-8

About Two Mechanisms of Reunion of Chaotic Attractors

YURI MAISTRENKO and IRINA SUSHKO

Institute of Mathematics National Academy of Sciences of Ukraine, Kiev, Ukraine

and

LAURA GARDINI†

Dipartimento di Metodi Quantitativi, University of Brescia, and Istituto di Scienze Economiche, University of Urbino, 61029 Urbino, Italy

(Accepted 24 February 1998)

Abstract—Considering a family of two-dimensional piecewise linear maps, we discuss two different mechanisms of reunion of two (or more) pieces of cyclic chaotic attractors into a one-piece attracting set, observed in several models. It is shown that, in the case of so-called 'contact bifurcation of the 2^{nd} kind', the reunion occurs immediately due to homoclinic bifurcation of some saddle cycle belonging to the basin boundary of the attractor. In the case of so-called 'contact bifurcation of the 1^{st} kind', the reunion is a result of a contact of the attractor with its basin boundary which is fractal, including the stable set of a chaotic invariant hyperbolic set appeared after the homoclinic bifurcation of a saddle cycle on the basin boundary. © 1998 Elsevier Science Ltd. All rights reserved.

1. INTRODUCTION

Our purpose is to describe some mechanisms of reunion of two or more pieces of a cyclic chaotic attractor in R^2 into a one-piece chaotic attracting set.

When observing such a reunion in several nonlinear models, one can often classify it in one of the following two possibilities:

1. It is due to a so-called 'contact bifurcation of the 2^{nd} kind' [1–4], giving rise to a direct reunion of the pieces of the attractor by pairs, and the resulting shape of the attractor is a junction, two by two, of the pieces existing before separately (Fig. 1).
2. Another type of reunion is due to a so-called 'contact bifurcation of the 1^{st} kind' (see the same references as above): two or more pieces of some cyclic chaotic attractor, being situated far enough from each other, under small parameter variation, can suddenly give rise to the appearance of bursts—rare points of the trajectories in some region of the phase space including the old pieces of attractors [Fig. 2(a)]. The number of the rare points increases as the iterations are continued, and they belong to a new chaotic attractor [Fig. 2(b)]. In some sense, chaotic attractors begin to 'feel each other' when the distance between them is still finite. When calculating trajectories in a system with 'rare points', their appearance seems rather unusual as we cannot see, in phase space, any other attracting set except for the two

†Author for correspondence

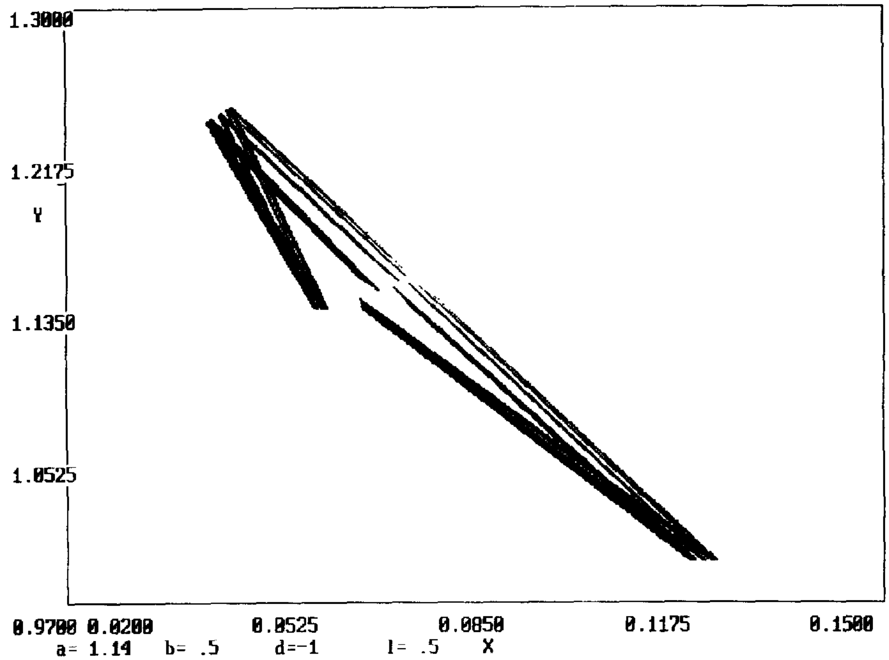

Fig. 1. An example of the "contact bifurcation of the 2^{nd} kind" when the reunion of two pieces of an attractor occurs due to the first homoclinic bifurcation of a saddle cycle belonging to the basin boundary of the attractor.

(or more) pieces of attractor under consideration. Due to this, it can be supposed that, in the region between the attractors, a repeller should exist. Contact bifurcation with it causes the rare points. Moreover, such repeller have a complicated topological structure, so that an observer cannot usually see any order in the appearance of such rare points and this visual randomness has both phase space and temporal nature.

Really, as described in [4] (ch. 5), besides the two types recalled above, there are several kinds of contact bifurcations between chaotic attractors and their basins, with different dynamical effects. However, we shall restrict our interest to the two mentioned above, because these are the two kinds of contact bifurcations involved in the piece-wise linear maps which interest us in this work.

The family F of maps that we consider is the family of two-dimensional piecewise linear continuous maps, as a function of four parameters, given by:

$$F = \begin{cases} F_1: \begin{pmatrix} x \\ y \end{pmatrix} \mapsto \begin{pmatrix} l & 0 \\ 0 & a \end{pmatrix} \begin{pmatrix} x \\ y \end{pmatrix}, & y \leq x+1, \\ F_2: \begin{pmatrix} x \\ y \end{pmatrix} \mapsto \begin{pmatrix} l-b & b \\ a-d & d \end{pmatrix} \begin{pmatrix} x \\ y \end{pmatrix} + \begin{pmatrix} -b \\ a-d \end{pmatrix}, & y \geq x+1, \end{cases} \tag{1}$$

where both the above mentioned scenarios can be realized, depending on the parameters of the family. Note that the map F can be considered in some sense as a 2Dim analog of the skew tent map. We shall consider the case in which F has two saddle fixed points, O and P, which are at the boundary of a closed bounded trapping region, Z, of the phase plane (where trapping means mapped into itself: $F(Z) \subseteq Z$).

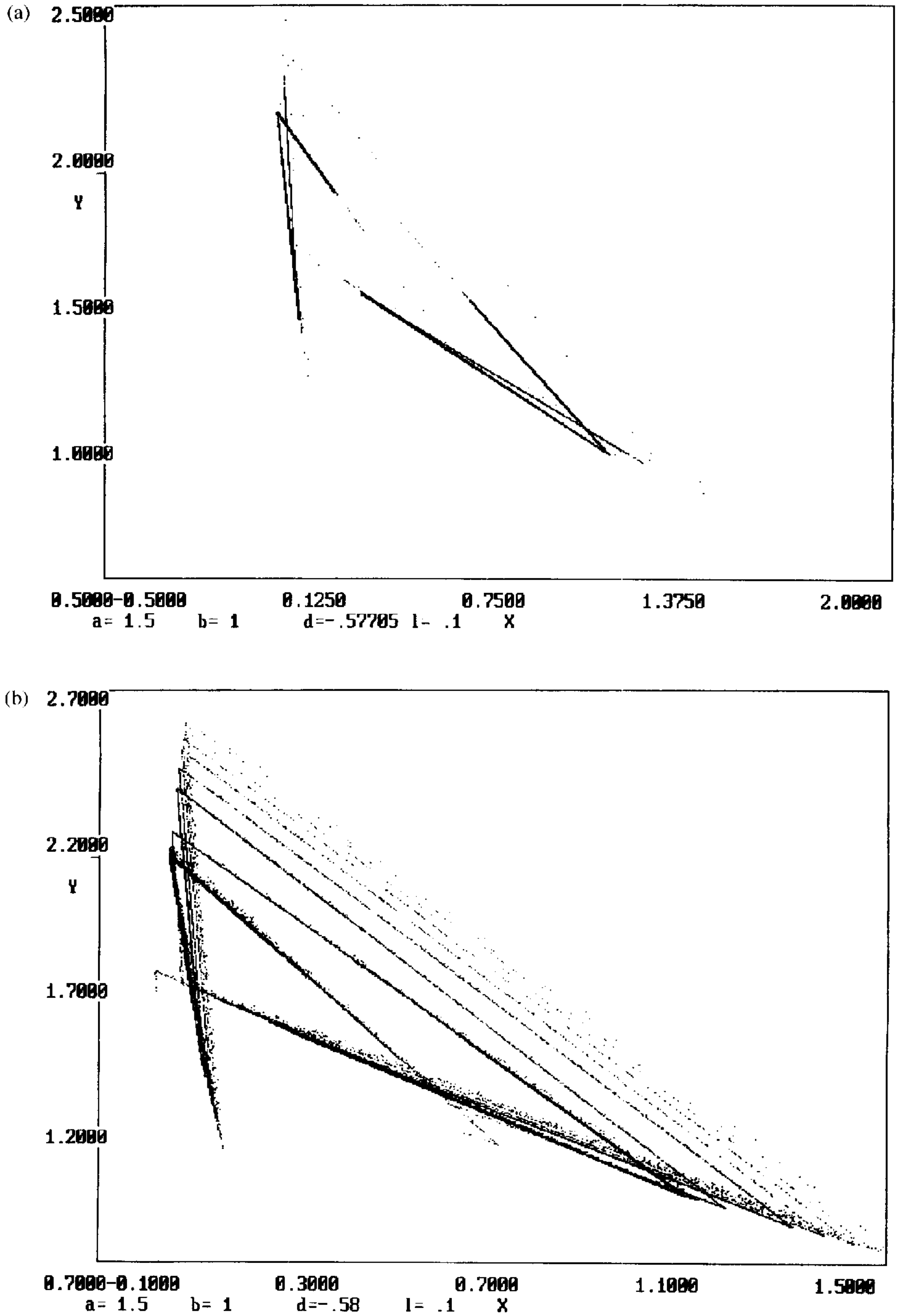

Fig. 2. An example of "contact bifurcation of the 1st kind" when the reunion of two pieces of an attractor is via appearance of rare points of the trajectories in the regions between pieces, when they are still far from each other. The reunion occurs due to a boundary crisis: each chaotic piece has a contact with its fractal basin boundary.

It should be noted that the case in which a dynamical system has two saddle fixed points occurs quite often in the modern theory of nonlinear dynamics.

We shall see that, in the first case, the contact bifurcation (without rare points) is a result of the first homoclinic bifurcation of the saddle P. In the second case, the reunion bifurcation (with rare points) is caused by the contact of the attractors with the boundary of its basin of attraction, which includes the stable set of the saddle P after its first homoclinic bifurcation.

Therefore, two different situations can occur in our model: in the first case, the first homoclinic bifurcation of P gives rise to immediate reunion of the attractors. In the second one, the homoclinic bifurcation of the saddle P creates an hyperbolic invariant set Λ (on the boundary of the basins) without reunion of attractors. The stable set $W^s(\Lambda)$ of the set Λ has Cantor like structure. It plays the role of 'separator' of the basins of the different pieces of the cyclic attractor. Under parameter variation, a bifurcation occurs when the chaotic attractors have a contact with $W^s(\Lambda)$. At this bifurcation value, the basin of each piece of the cyclic attractor comes to be intermingled, assuming that the preimages of each contact point are dense everywhere on the 'attractor'. Soon after the contact bifurcation, the old attractor disappears due to the infinitely many intersections with $W^s(\Lambda)$, and a new attractor arises.

The structure of the paper is as follows. In Section 2, we describe the map F. A so-called 'saddle–saddle' area is defined in the parameter space when both the fixed points of the map F are saddles. Correspondingly, a bounded invariant area is found in the phase space.

Section 3 is devoted to the study of different kinds of attractors of the map F. Depending on the parameters, the attractor can be either a cycle of any period or a cyclic chaotic attractor of any period. We give exact formulae for the boundaries of the regions of existence of the attracting cycles of different periods. A conjecture is formulated about the order of appearance of the attractors in the system under parameter variation. It is shown that the case of stability loosing of any point cycle due to the flip bifurcation (besides the cycle of period 2) results in the appearance of a cyclic chaotic attractor of doubling period. In the case in which the cycle of period 2 becomes unstable, a cyclic chaotic attractor of period 2^i can appear, where i depends on the parameters. The bifurcations which may then occur consists of the pairwise reunion of the pieces of the attractor to give only a one-piece chaotic set. The main problem concerns the bifurcation causing the reunion. It is connected with the first homoclinic bifurcation of the saddle P (Section 4) as well as with an invariant hyperbolic set analogous to the Smale horseshoe which appears after the homoclinic bifurcation. We give a construction of this set in Section 6.

Different mechanisms of reunion of pieces of cyclic chaotic attractors are explained in Section 5, considering the sequences of bifurcations of the 4-, 2- and 1-piece chaotic attractors, as well as those of the 6-, 3- and 1-piece chaotic attractors.

2. DESCRIPTION OF THE MAP. 'SADDLE–SADDLE AREA' IN THE PARAMETER SPACE. BOUNDED INVARIANT REGION IN THE PHASE SPACE

Consider the four-parameter family F of two-dimensional piecewise linear continuous maps given in (1). The map F consists of two linear maps F_1 and F_2 defined below and above, respectively, the straight line $LC_{-1} = \{(x,y):y = x+1\}$ which is a line of discontinuity of the Jacobian of the map, F. The map, F, is one-to-one if $d > ab/l$ and is noninvertible otherwise. Indeed, if $d < ab/l$, the map, F, is of $(Z_0 - Z_2)$ type, i.e. each point $(x,y) \in R^2$ has two preimages, provided that $y < ax/l + a$; has zero preimages, provided that $y > ax/l + a$ and has a unique preimage if $y = ax/l + a$. Thus, the straight line, $LC = \{(x,y):y = ax/l + a\}$, is the locus of 'critical values' of F, i.e. the so-called critical line of rank-1 [5, 2, 4]. Due to these properties, the map F can be considered as a two-dimensional analog of the skew tent map.

Denote the fixed point of F_1 by $O = (0,0)$. The eigenvalues of F_1 are

$$\mu_1 = a \text{ and } \mu_2 = l$$

with corresponding eigendirections

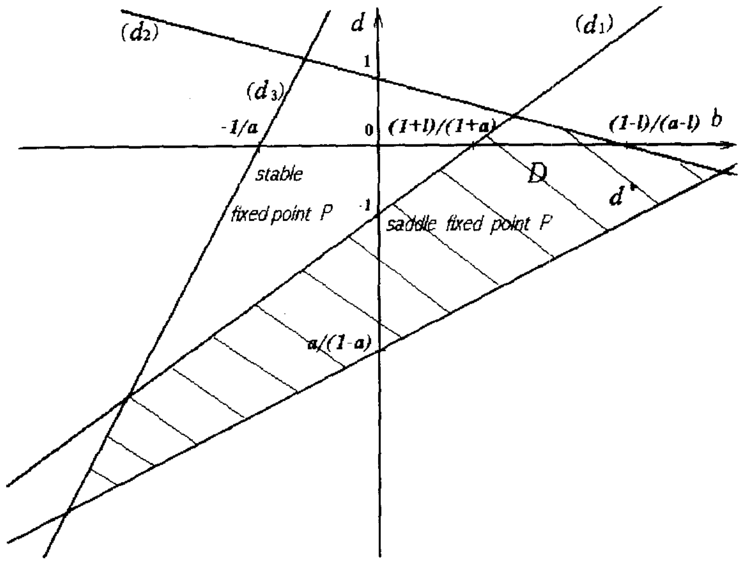

Fig. 3. The triangle of stability of the fixed point P in the (b, d)-parameter plane, $a > 1$, $0 < l < 1$; D is the region in which P is saddle.

$$u_1 = (0,1) \text{ and } u_2 = (1,0).$$

Let us fix the parameters a and l so that the fixed point O is a saddle:

$$a > 1,\ \ 0 < l < 1.$$

The local stable (unstable) manifold of O is denoted by $w_0(O)$ ($\alpha_0(O)$) which is obviously a segment of the straight line $\{y = 0\}$ ($\{x = 0\}$).

The fixed point of the map F_2 is denoted by $P = (x_0, y_0)$, where

$$x_0 = \frac{b(1-a)}{b(a-1)-(1-d)(1-l)};\ y_0 = \frac{(1-l)(d-a)}{b(a-1)-(1-d)(1-l)}.$$

We are interested in a so-called 'saddle–saddle' area D in the parameter space in which both the fixed points O and P are saddles and, moreover, a bounded trapping region Z exists in the phase plane (x,y).

For any fixed $a > 1$ and $0 < l < 1$, the region of stability of $P = (x_0, y_0)$ in the (b,d) parameter plane is the triangle Π_1 bounded by three segments of the following straight lines

$$d = -1 + b(1+a)/(1+l), (d_1)$$

$$d = 1 + b(1-a)/(1-l), (d_2)$$

$$d = (ab+1)/l, (d_3)$$

The fixed point P becomes a saddle if the parameter point (b,d) intersects either (d_1) (the eigenvalue of P crosses through -1) or (d_2) (the eigenvalue crosses through 1). In the last case, obviously a bounded invariant area in the phase plane does not exist. Thus, the region D, in the parameters' space we are interested in is defined as follows:

$$D = \{(a,b,d,l)\colon a > 1,\ d^* < d < \min_{b \in R^1}\{(d_1),(d_2),(d_3)\}, 0 < l < 1\}$$

where d^* denotes a bifurcation curve of destruction of the trapping region Z which will be defined below (Fig. 3). We will restrict ourself to the condition $b > 0$ (at $b = 0$, the map F is a triangular map and its dynamics are described in [8]).

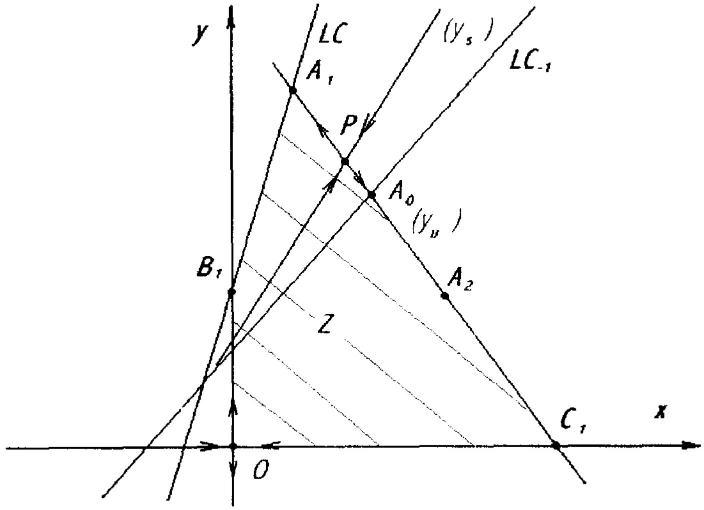

Fig. 4. Trapping region Z of the map F, in the phase plane (x, y).

The local stable (unstable) manifold of P is denoted by $w_0(P)$ $(\alpha_0(P))$ which is a segment of the straight line $y = Q^s x + R^s$ denoted as (y_s) for short, $(y = Q^u x + R^u$, denoted as (y_u) for short) where

$$Q^s = \frac{\lambda_1 + b - l}{b};\ R^s = \frac{d(1-l) - (\lambda_1 + b)(1-a) + l - a}{ba - dl + d + l - b - 1};$$

$$Q^u = \frac{\lambda_2 + b - l}{b};\ R^u = \frac{d(1-l) - (\lambda_2 + b)(1-a) + l - a}{ba - dl + d + l - b - 1};$$

and $0 < \lambda_1 < 1$, $\lambda_2 < -1$ are eigenvalues of F_2:

$$\lambda_1 = (l - b + d + \sqrt{(b - l - d)^2 - 4(dl - ba)})/2,$$

$$\lambda_2 = (l - b + d - \sqrt{(b - l - d)^2 - 4(dl - ba)})/2.$$

Assuming now that the parameters belong to the region D, we shall find a bounded region in the phase plane (x,y) which is trapping for F. Consider the region Z, bounded by the segments of the four straight lines: $\{x = 0\}$, $\{y = 0\}$ (containing, respectively, $\alpha_0(O)$ and $w_0(O)$), LC and of the straight line (y_u) (containing $\alpha_0(P)$). The region Z is a quadrilateral with corner points $O = (0,0)$, $A_1 = LC \cap (y_u)$, $B_1 = (0,a)$ and $C_1 = (-R^u/Q^u, 0)$ (Fig. 4). It is easy to see that if $(a,b,d,l) \in D$ and $b > 0$ then the region Z is trapping (i.e. mapped into itself: $F(Z) \subseteq Z$). The bifurcation destroying the invariance of Z takes place when $F_2(A_1) = C_1$. This bifurcation determines the appearance of the first heteroclinic trajectory from the saddle P to the saddle O and also the homoclinic connection for O (see [2, 4]). The curve d^* in the parameter space corresponds to this last condition.

3. ATTRACTORS: ATTRACTING CYCLES AND CYCLIC CHAOTIC ATTRACTORS

Let $(a,b,d,l) \in D$, $b > 0$ and, consequently, the bounded invariant region Z exists in the phase plane. We shall see that an attractor of the map F, necessarily belonging to Z, is either an attracting cycle γ_n of period n or a cyclic chaotic attractor $A_{n,m}$ of period m, where n, m can assume any natural value, depending on the parameters.

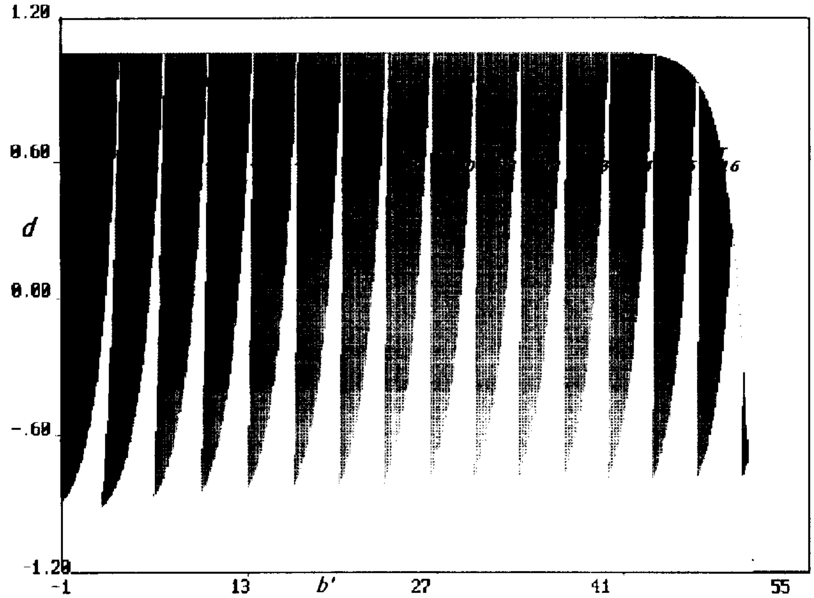

Fig. 5. The regions Π_n of existence of attracting cycles γ_n in the (b', d)-parameter plane where $b' = 2^b$, at $a = 1 + 10^{-5}$ and $l = 0.3$ for $n = 2, \ldots, 17$.

We shall find the regions $\Pi_n \in D$, $n \geq 2$, such that if parameters belong to Π_n, then an attracting cycle of period n of the map F exists. Let $\gamma_n = \{(x_1,y_1),(x_2,y_2),\ldots,(x_n,y_n)\}$ be a cycle of period n such that one of its points (let us assume the point (x_1,y_1)) belongs to the region $x+1<y<ax/l+a$, i.e., $x_1+1<y_1<ax_1/l+a$; and the other points belong to the region $0<y<x+1$, i.e., $0<y_i<x_i+1$, $i = 2,\ldots, n$. The appearance of γ_n is a result of saddle–node bifurcation and it is defined by the condition $(x_1,y_1) \in LC$. From $(x_1,y_1) = F_1^{n-1}(F_2(x_1,y_1))$ at $y_1 = ax_1/l+a$ we get the locus, in the parameter space, of the appearance of γ_n:

$$d_{n,e} = \frac{bl^{n-2}(1-l)(a^n-1)+(l^n-1)(a^{n-1}-1)}{a^{n-2}(a-1)(1-l^n)},$$

which is a straight line in the (b,d) parameter plane at fixed values for a, l and n. Note that the cycle γ_2 arises at the stability loosing of the fixed point P, that is $d_{2,e} = (d_1)$.

The curve of stability loosing of γ_n can be found as a result of flip bifurcation, when one of the cycle multiplicators becomes equal to -1. Also, this curve is a straight line in the (b,d) parameter plane at fixed a, l and n:

$$d_{n,s} = -\frac{1}{a^{n-1}} + \frac{bl^{n-1}(a^n+1)}{a^{n-1}(l^n+1)}.$$

Thus, the regions $\Pi_n \in D$ of existence of attracting cycles γ_n are:

$$\Pi_n = \{(a,b,d,l) \in D : d_{n,s} < d < d_{n,e}\}.$$

The regions Π_n are shown in Fig. 5 in the (b',d) parameter plane where $b' = 2^b$ at $a = 1+10^{-5}$, $l = 0.3$ where $n = 2,\ldots, 17$.

Note that, at fixed values, $a>1$, $0<l<1$, the number of the regions Π_n is finite, that is $n = 2,\ldots, n^*$, where n^* is a number which depends on a and l. Moreover, if $al>1$, there is not any attracting cycle of the map F at $(a,b,d,l) \in D$. But, if $a \to 1$ and $l \to 1$, then $n^* \to \infty$.

When the parameter point (b,d) crosses one of the regions Π_n through the curve $d_{n,s}$, a flip bifurcation for γ_n occurs. What is the result for the dynamics of the map F? Computer simulations show that this bifurcation gives rise to the appearance of a cyclic chaotic attractor, of doubling period $2n$ when $n \geq 3$ and of period 2^k for $n = 2$, k depending on the parameters. Further variation of the parameters can give rise to the bifurcation of the pairwise reunion of the pieces of the attractor and, finally, all pieces merge into a one-piece attracting set.

By $\mathcal{A}_{n,m}$, we denote a cyclic chaotic attractor of period m, arising after stability loosing of the cycle of period n. Using analytical results and computer simulations, we can deduce the following consequences for the bifurcations under parameters variation:

1. Let $n = 2$:

$$\gamma_2 \Rightarrow \mathcal{A}_{2,2^k} \Rightarrow \mathcal{A}_{2,2^{k-1}} \Rightarrow \ldots \Rightarrow \mathcal{A}_{2,2} \Rightarrow \mathcal{A}_{2,1},$$

where k can be any positive integer depending on the parameters, moreover, $k \to \infty$, as $a \to 1$, $b \to 0$, $d \to -1$ and $l \to 0$.

2. Let $n \geq 3$:

$$\gamma_n \Rightarrow \mathcal{A}_{n,2n} \Rightarrow \mathcal{A}_{n,n} \Rightarrow \mathcal{A}_{n,1}.$$

As was mentioned above, the bifurcations $\gamma_2 \Rightarrow \mathcal{A}_{2,2^k}$ and $\gamma_n \Rightarrow \mathcal{A}_{n,2n}$ are flip bifurcations for the corresponding cycles (γ_2 and γ_n). Our purpose is to describe the bifurcations causing the reunion of the pieces of the cyclic chaotic attractors, i.e. bifurcations $\mathcal{A}_{n,2n} \Rightarrow \mathcal{A}_{n,n}$, $\mathcal{A}_{n,n} \Rightarrow \mathcal{A}_{n,1}$, $\mathcal{A}_{2,2^i} \Rightarrow \mathcal{A}_{2,2^{i-1}}$, $i = 2, \ldots, k$.

4. STRUCTURE OF STABLE AND UNSTABLE SETS OF *P*. FIRST HOMOCLINIC BIFURCATION OF *P*

In order to describe the first homoclinic bifurcation of the saddle fixed point P, we consider the structure of its stable and unstable sets. The stable set of P has the form:

$$W^s(P) = w_0(P) \cup \bigcup_{n \geq 1} F^{-n}(w_0(P)) = w_0(P) \cup \bigcup_{n \geq 1} w_{-n}^{i_1 \ldots i_n}, i_1 = 1; i_2, \ldots, i_n = 1,2,$$

where $w_0(P)$ is the local stable set of P, that is, a halfline of equation (y_s) with the end point $W_0 = LC \cap (y_s)$. The global stable set $W^s(P)$ is given by the union of all the preimages of $w_0(P)$:

$$F^{-1}(w_0) = F_1^{-1}(w_0) \cup F_2^{-1}(w_0) = w_0 \cup w_{-1}^1$$

where the set $w_0 \cup w_{-1}^1$ consists of two half-lines issuing from the point W_{-1} (see Fig. 6a),

$$F^{-2}(w_0) = F_1^{-1}(w_{-1}^1) \cup F_2^{-1}(w_{-1}^1) = w_{-2}^{11} \cup w_{-2}^{12},$$

$$F^{-3}(w_0) = F^{-1}(w_{-2}^{11}) \cup F^{-1}(w_{-2}^{12}) = w_{-3}^{111} \cup w_{-3}^{112} \cup w_{-3}^{122} \cup w_{-3}^{121},$$

$$F^{-4}(w_0) = F^{-1}(w_{-3}^{111}) \cup F^{-1}(w_{-3}^{112}) \cup F^{-1}(w_{-3}^{122}) \cup F^{-1}(w_{-3}^{121})$$

$$= w_{-4}^{1111} \cup w_{-4}^{1112} \cup w_{-4}^{1121} \cup w_{-4}^{1122} \cup w_{-4}^{1221} \cup w_{-4}^{1222} \cup w_{-4}^{1212} \cup w_{-4}^{1211},$$

and so on. By *main beak* we shall call the beak formed by the halflines w_{-3}^{121} and w_{-3}^{122} with the end point C_{-3} where $C_{-3} = F_2^{-1} F_1^{-1}(C_{-1})$, $C_{-1} = w_{-1}^1 \cap LC_1$ [see Fig. 6(a)].

The unstable set of P is given by:

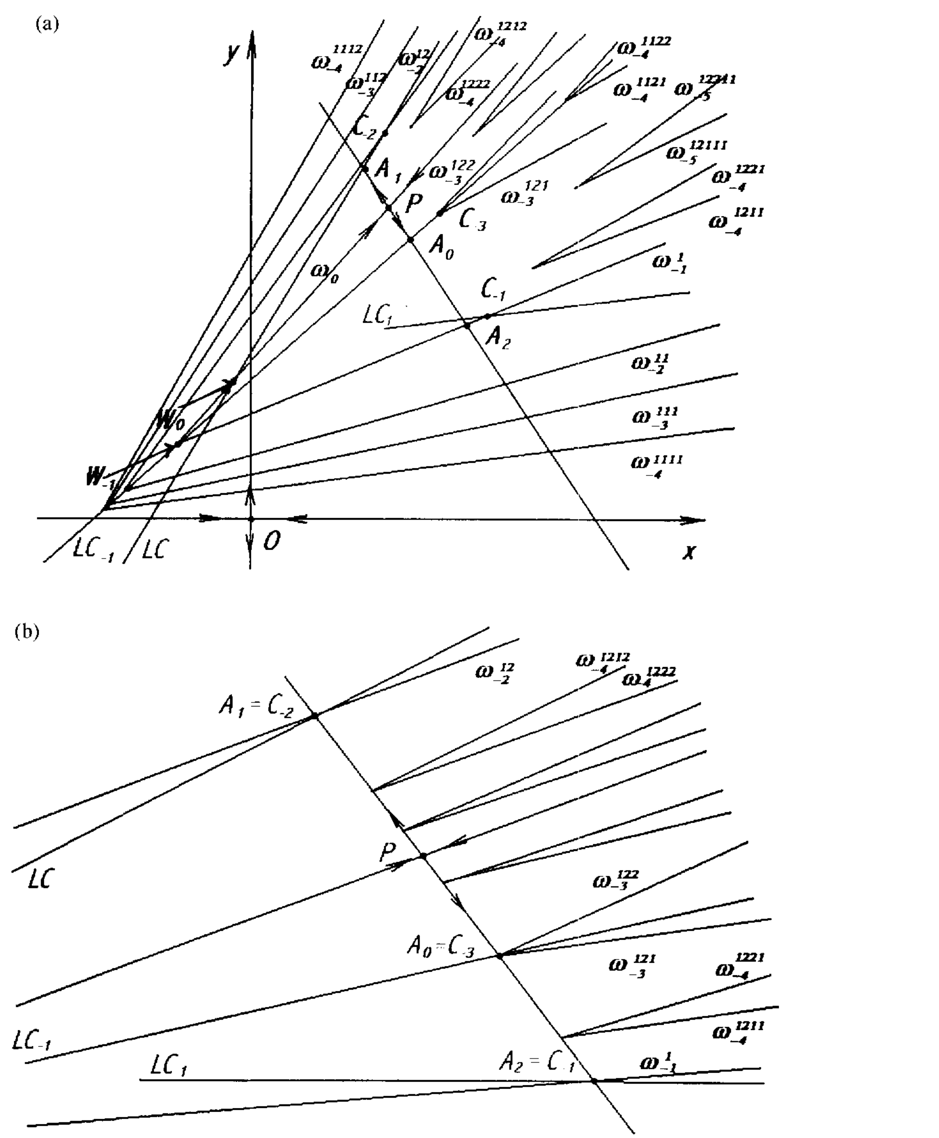

Fig. 6. The structure of the stable set $W^s(P)$ of the saddle fixed point P before (a) and in the moment (b) of the first homoclinic bifurcation of P.

$$W^u(P) = \alpha_0(P) \cup \bigcup_{n \geq 1}^{\infty} F^n(\alpha_0(P)),$$

where $\alpha_0(P)$ is the local unstable manifold of P, given by the segment $[A_1, A_2]$, where $A_1 = F(A_0)$, $A_0 = LC_{-1} \cap (y_u)$, $A_2 = F_2(A_1)$.

The first homoclinic bifurcation of P occurs when $C_{-3} = A_0$ (which corresponds also to the merging of C_{-2} with A_1 and C_{-1} with A_2), i.e. when the main beak (and thus the stable set of P) has a first contact with $W^u(P)$ and, consequently, infinitely many preimages of the main beak also have the contacts with $W^u(P)$ [see Fig. 6(b)]. The curve $\mathscr{H}$ in the parameter plane (b,d) corresponding to the first homoclinic bifurcation of P is shown in Fig. 7, as well as the curves $\mathscr{H}_{2^i}$, $i = 1,..\ 4$, corresponding to the first homoclinic bifurcations of saddle cycles of period 2^i,

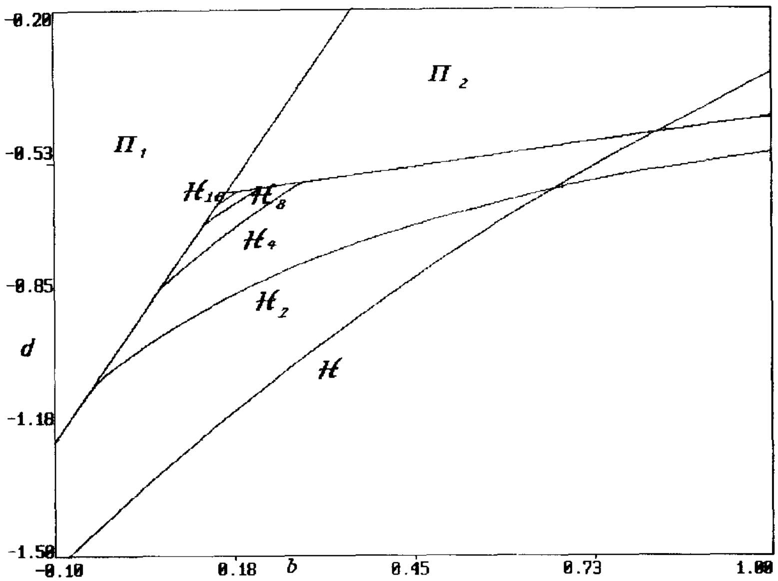

Fig. 7. The curve $\mathcal{H}$, in the parameter plane (b, d), of the first homoclinic bifurcation of P. The curves $\mathcal{H}_{2^i}$, $i = 1,\ldots,4$ of the first homoclinic bifurcations of period-2^i saddle cycles such that a half of the cycle points lie above LC_{-1} and the others are below. Each curve $\mathcal{H}_{2^i}$ correspond to the bifurcation of pairwise reunion of the pieces of the cyclic chaotic attractor $\mathcal{A}_{2,2^{i+1}} \Rightarrow \mathcal{A}_{2,2^i}$.

such that half of the cycle points lie above LC_{-1} and the others are below. The curves $\mathcal{H}_{2^i}$ separate the regions of existence of the cyclic chaotic attractors $\mathcal{A}_{2,2^{i-1}}$ of period 2^{i-1} and $\mathcal{A}_{2,2^i}$ of period 2^i, i.e. corresponding to the bifurcation of pairwise reunion of the pieces of the cyclic chaotic attractor: $\mathcal{A}_{2,2^{i+1}} \Rightarrow \mathcal{A}_{2,2^i}$. While for the curve $\mathcal{H}$, as we will see, for some parameter values, it also corresponds to the reunion of two pieces of the chaotic attractor into a one-piece attractor, while for other parameter values, the homoclinic bifurcation of P does not cause such bifurcation in the attractor. In order to simplify the exposition, let us study in detail these two different cases considering the bifurcations $\mathcal{A}_{2,4} \Rightarrow \mathcal{A}_{2,2}$ and $\mathcal{A}_{2,2} \Rightarrow \mathcal{A}_{2,1}$.

5. TWO DIFFERENT MECHANISMS FOR THE REUNION OF TWO PIECES OF THE 2-CYCLIC CHAOTIC ATTRACTOR INTO A ONE-PIECE ATTRACTOR AND OF THREE PIECES OF THE 3-CYCLIC CHAOTIC INTO A ONE-PIECE ATTRACTOR

Let us fix the parameter values $a = 1.5$, $l = 0.1$, $b = 0.45$ and vary the parameter d starting from $d_1 = -0.7$. As can be seen from Fig. 7, at such parameter values, the dynamical system generated by F has a cyclic chaotic attractor $\mathcal{A}_{2,4}$ of period 4: $\mathcal{A}_{2,4} = \{\mathcal{A}^1_{2,4}, \mathcal{A}^2_{2,4}, \mathcal{A}^3_{2,4}, \mathcal{A}^4_{2,4}\}$; $F(\mathcal{A}^i_{2,4}) = \mathcal{A}^{i+1}_{2,4}$, $i = 1,2,3$, $F(\mathcal{A}^4_{2,4}) = \mathcal{A}^1_{2,4}$ (Fig. 8).

Using the theory of critical lines [5], we can find the boundary of the basin of attraction of each element $\mathcal{A}^i_{2,4} \subset \mathcal{A}_{2,4}$ with respect to the fourth iteration of F (see [2, 4] for details). Indeed, the immediate basin of attraction of $\mathcal{A}^1_{2,4}$ is bounded by the segments of the critical line LC, the local unstable manifold $\alpha_0(P)$ of P, as well as the local stable and unstable manifolds of the point p_1 which is one of the points of the saddle cycle $\gamma_2 = \{p_1, p_2\}$ of period 2. The first homoclinic bifurcation of γ_2 occurs at $d = -0.718\ldots$, giving rise to the pairwise reunion of $\mathcal{A}^i_{2,4}$ ($\mathcal{A}^1_{2,4}$ with $\mathcal{A}^3_{2,4}$ and $\mathcal{A}^2_{2,4}$ with $\mathcal{A}^4_{2,4}$). The result of the reunion is the cyclic chaotic attractor $\mathcal{A}_{2,2}$ of period 2: $\mathcal{A}_{2,2} = \{\mathcal{A}^1_{2,2}, \mathcal{A}^2_{2,2}\}$ (Fig. 9). Note that all the bifurcations $\mathcal{A}_{2,2^k} \Rightarrow \mathcal{A}_{2,2^{k-1}}$, $k = 3,\ldots$, are

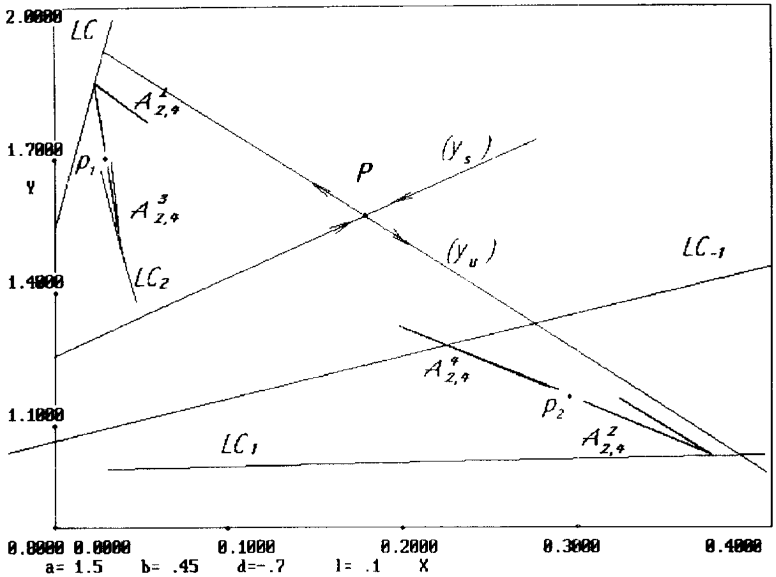

Fig. 8. A 4-cyclic chaotic attractor, $\mathscr{A}_{2,4} = \{\mathscr{A}^1_{2,4}, \mathscr{A}^2_{2,4}, \mathscr{A}^3_{2,4}, \mathscr{A}^4_{2,4}\}$ of the map F.

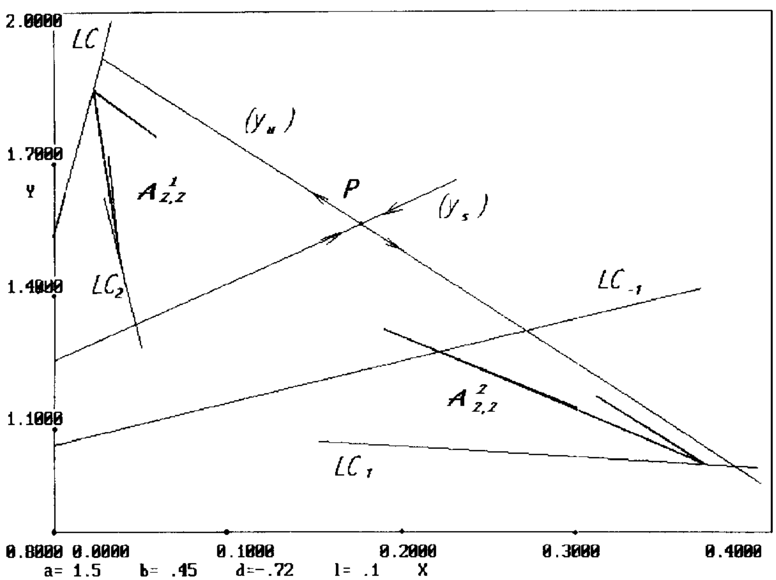

Fig. 9. A 2-cyclic chaotic attractor $\mathscr{A}_{2,2} = \{\mathscr{A}^1_{2,2}, \mathscr{A}^2_{2,2}\}$ of the map F.

analogous to the one described above, being the result of homoclinic bifurcation of the period -2^{k-1} saddle cycle.

Let us consider the last bifurcation $\mathscr{A}_{2,2} \Rightarrow \mathscr{A}_{2,1}$. The parameter point (b,d) intersects the curve $\mathscr{H}$ at $d = -0.835...$, and the first homoclinic bifurcation of P takes place (Fig. 10). As in the previous cases, the bifurcation causes the reunion of the pieces of the attractor $\mathscr{A}^1_{2,2}$ and $\mathscr{A}^2_{2,2}$ giving rise to the one-piece attracting set $\mathscr{A}_{2,1}$. Let us now consider a different crossing of the curve $\mathscr{H}$, in another point: $d = -0.53...$, $b = 0.8$. As can be seen from numerical experiments,

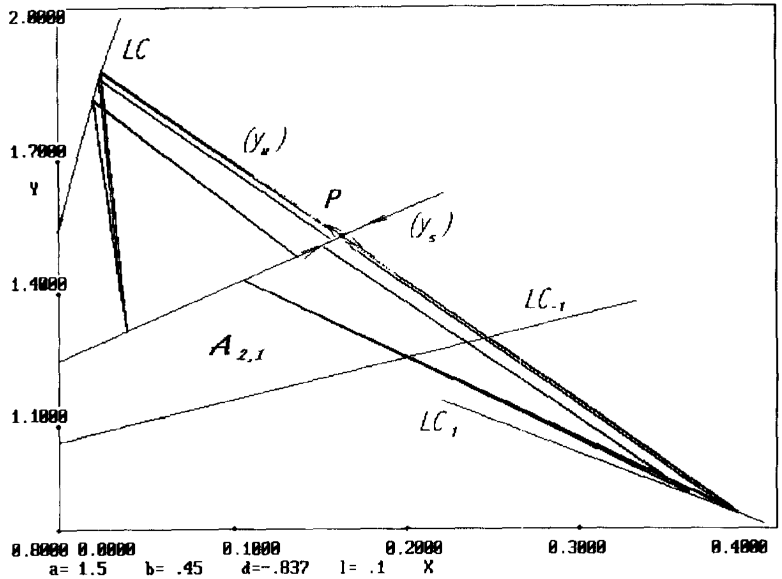

Fig. 10. Contact bifurcation of the 2^{nd} kind corresponding to the reunion of two pieces of the attractor $\mathcal{A}_{2,2}$ into a one-piece chaotic attractor $\mathcal{A}_{2,1}$.

in this case the homoclinic bifurcation of P does not cause the reunion of $\mathcal{A}^1_{2,2}$ with $\mathcal{A}^2_{2,2}$. After this bifurcation, as we shall see in Section 6, an invariant hyperbolic set Λ appears in the neighborhood of P. The stable set $W^s(\Lambda)$ of this set has a Cantor like structure and is a limit set of the stable set of P. It plays the role of 'separator' of the basins of the two disjoint attractors of the map F^2. Thus the basin boundary becomes a fractal set at this homoclinic bifurcation of P. In Fig. 11, the 2-piece attractor $\mathcal{A}_{2,2}$ and some branches of $W^s(P)$ are shown at $d = -0.55$, $b = 1$, at parameter values just beyond the first homoclinic bifurcation of P.

At $d = -0.57703...$ the attractor $\mathcal{A}_{2,2}$ has a first contact with $W^s(\Lambda)$. It is clear that such a contact shall cause the destruction of the closed invariant chaotic set, assuming that the preimages of the contact point are dense everywhere on the attractor. Just after this bifurcation, numerical evidence shows the existence of an attractor with a high density of iterated points in the places previously occupied (i.e. before the contact) by the old two pieces of the attractor and rare iterated points between them (Fig. 12). These rare points belong to the trajectories which escape through the gaps appearing after the intersection of the attractor with $W^s(\Lambda)$. They spend a relatively short time all over the attractor, following the unstable set of P, then return again inside the old position of the two-piece attractor and remain there for a sufficiently long time. And so on. Indeed, we already get a one-piece attractor $\mathcal{A}_{2,1}$. If we continue to iterate, the new shape of the attractor comes to be close to the unstable set $W^u(P)$ [see Fig. 2(b)].

When considering the curve $\mathcal{H}$, one can find a point h separating two different kinds of mechanisms of reunion of two pieces of $\mathcal{A}_{2,2}$ as described above: a crossing of $\mathcal{H}$ to the left of h gives rise to the immediate reunion at the moment of homoclinic bifurcation of P; to the right side of h, the homoclinic bifurcation results in basin fractalization only and the real curve of merging of the two pieces of the attractor, starting from the h, lies below $\mathcal{H}$. It is a curve characterized by the contact of the attractor with its basin boundary.

Above, we have considered the consequence of bifurcations $\mathcal{A}_{4,2} \Rightarrow \mathcal{A}_{2,2} \Rightarrow \mathcal{A}_{2,1}$, i.e. the reunion bifurcations for the pieces of the 2^i-cyclic chaotic attractor, $i = 1, \ldots, k$. We assume that, in the general case, $n \geq 3$ the bifurcation $\mathcal{A}_{n,2n} \Rightarrow \mathcal{A}_{n,n}$ is always of the 2^{nd} kind, i.e. the result of the

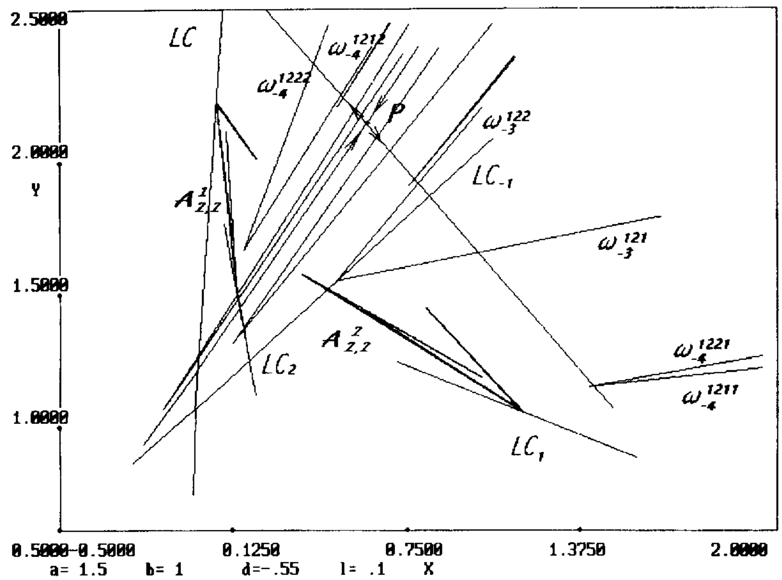

Fig. 11. An example of the 2-cyclic chaotic attractor $\mathcal{A}_{2,2} = \{\mathcal{A}^1_{2,2}, \mathcal{A}^2_{2,2}\}$ of the map F and some brunches of the stable set of the saddle P, after the first homoclinic bifurcation of P.

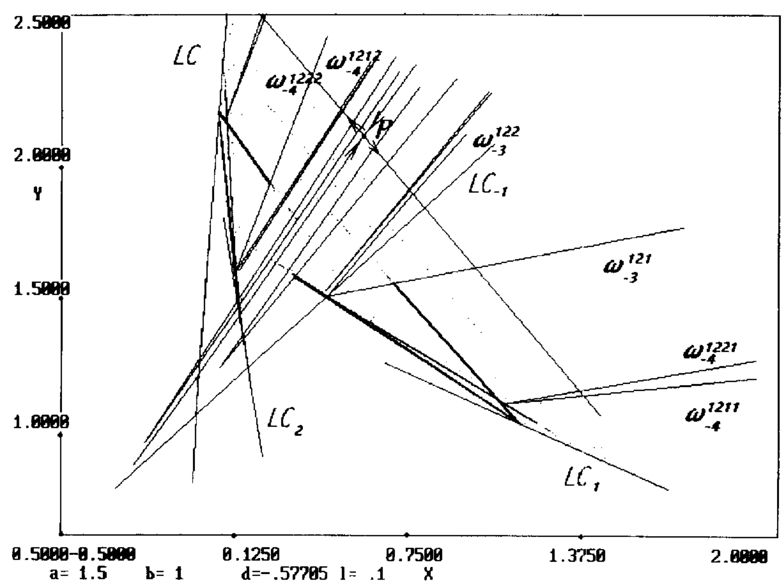

Fig. 12. Contact bifurcation of the 1^{st} kind corresponding to the reunion of two pieces of the attractor $\mathcal{A}_{2,2}$ into a one-piece chaotic attractor $\mathcal{A}_{2,1}$ via appearance of rare points of the trajectories in the regions between the pieces.

homoclinic bifurcation of the saddle cycle of period n on the basin boundary, while the bifurcation $\mathcal{A}_{n,n} \Rightarrow \mathcal{A}_{n,1}$ is always of the 1^{st} kind.

As an example, let us consider the sequence of bifurcations $\mathcal{A}_{3,6} \Rightarrow \mathcal{A}_{3,3}$ and $\mathcal{A}_{3,3} \Rightarrow \mathcal{A}_{3,1}$. In Fig. 13(a), the 6-cyclic chaotic attractor, $\mathcal{A}_{3,6}$, is shown at parameter values $a = 1.05$, $b = 4$, $d = -0.27$ and $l = 0.3$. This attractor appears after the flip bifurcation of the attracting cycle

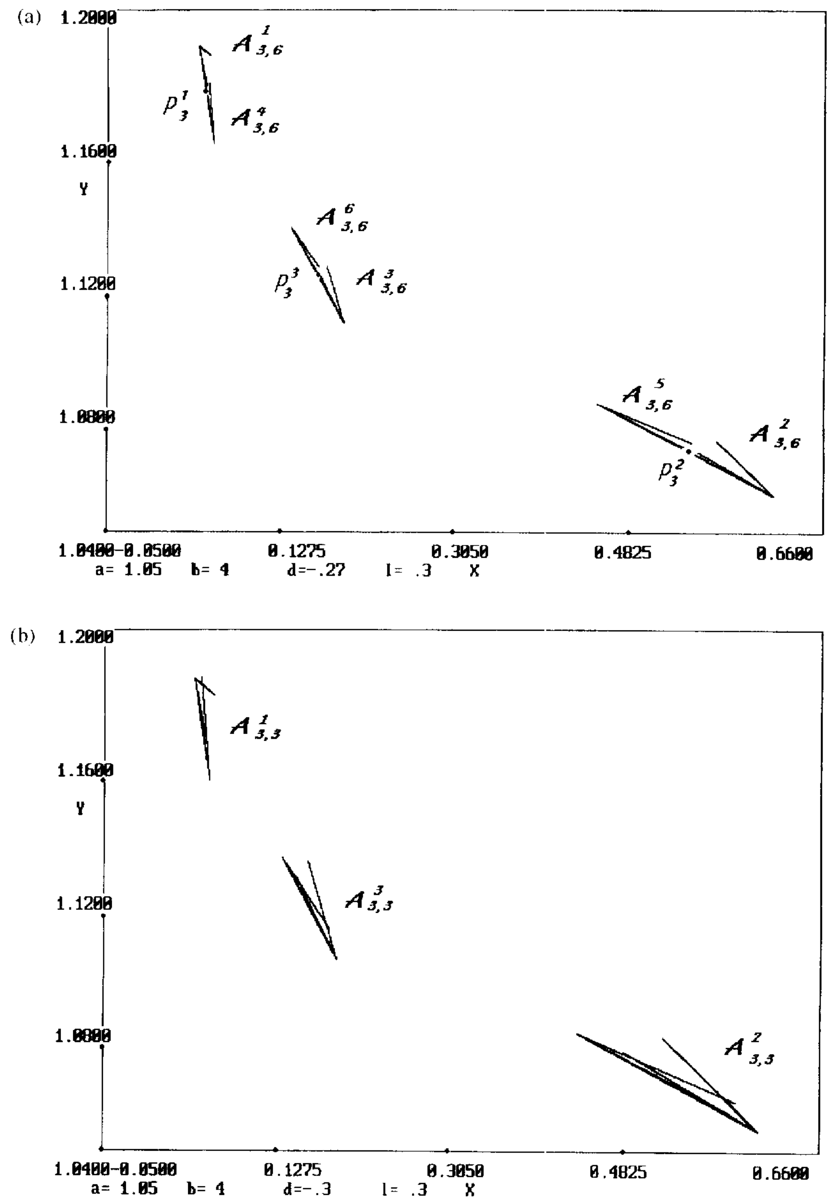

Fig. 13. A 6-cyclic chaotic attractor $\mathcal{A}_{3,6} = \{\mathcal{A}^1_{3,6}, \mathcal{A}^2_{3,6}, \ldots, \mathcal{A}^6_{3,6}\}$ of the map F (a) which bifurcates into the 3-cyclic chaotic attractor $\mathcal{A}_{3,3} = \{\mathcal{A}^1_{3,3}, \mathcal{A}^2_{3,3}, \mathcal{A}^3_{3,3}\}$ (b) due to the contact bifurcation of 2^{nd} kind. The one-piece chaotic attractor $\mathcal{A}_{3,1}$ (c) is obtained as a result of the contact bifurcation of 1^{st} kind.

$\gamma_3 = \{p^1_3, p^2_3, p^3_3\}$, which becomes a saddle. At $d = -0.29\ldots$ the attractor $\mathcal{A}_{3,6}$ bifurcates into the 3-cyclic chaotic attractor $\mathcal{A}_{3,3}$ [Fig. 13(b)] due to the contact bifurcation of the 2^{nd} kind, which corresponds to the first homoclinic bifurcation of the saddle cycle γ_3.

At $d = -0.315\ldots$, the one-piece chaotic attractor, $\mathcal{A}_{3,1}$ is obtained [Fig. 13(c)] as a result of the contact bifurcation of the 1^{st} kind, that is, the reunion of the three pieces of the attractor occurs due to the contact of each piece of the attractor with its basin boundary, which is already fractal.

(c)

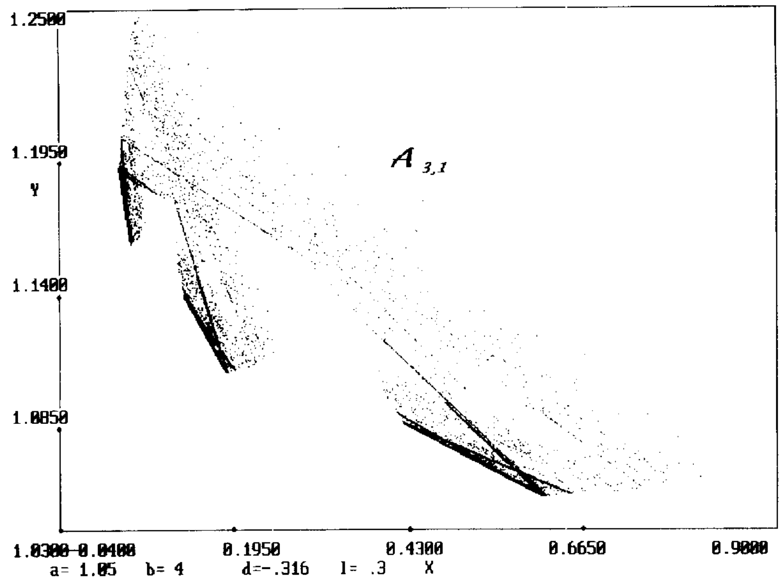

Fig. 13—*continued*.

6. DESCRIPTION OF THE HORSESHOE

In this section, we construct an invariant hyperbolic set analogous to the Smale horseshoe, which appears after the first homoclinic bifurcation of P. Let us consider the parameter values soon after this bifurcation of P (described by the curve $\mathscr{H}$ in Fig. 7), for example, by taking a lower value of d. Then the beaks belonging to the stable set of P will cross the unstable set of P, creating infinitely many homoclinic points of P. Our purpose is to show that, also in this case (our map F is not a diffeomorphism but a two-dimensional piecewise linear map with a non unique inverse), the existence of homoclinic points of P implies the existence of an hyperbolic Cantor set Λ, with chaotic dynamics, near P, for a suitable power of F, say F^m, and correspondingly, this gives an invariant chaotic set for the map F, called L in the previous sections. To see this, let us recall the 'folding' action of the critical curve LC. If we consider a strip S crossing LC_{-1}, as in Fig. 14(a) and one side along the unstable set $W^u(P)$ for convenience, then $F(S)$ is 'folded' along LC. Figure 14(a) also schematically shows the relative positions of the critical segments of interest with the stable and unstable sets of P. Note that $S_1 = F(S) = S^{(1)} \cup S^{(2)} = F_1(S \cap R_1) \cup F_2(S \cap R_2)$ and, for the non invertibility of F, we have $F^{-1}(S_1) \supset S$. However, we can recover S as follows: $F_1^{-1}(S^{(1)}) \cup F_2^{-1}(S^{(2)}) = S$. Note also that if we take the strip S crossing not only LC_{-1}, but also the two branches of ω_{-3} issuing from the point C_{-3} of LC_{-1} (see Fig. 14(a)), then $F(S)$ intersects ω_{-2}. Moreover, we can always take S in such a way that $F(S)$ intersects ω_{-2} in two disjoint segments, as in Fig. 14(a). In fact, we can proceed in reverse order, choosing $S^{(1)} \cup S^{(2)}$ first, as in Fig. 14(a), with disjoint intersections with ω_{-2}, and having two portions labelled π_1 and π_2 below ω_{-2}. Note that both π_1 and π_2 have one side bounded by a segment of $W^s(P)$, one side bounded by a segment of $W^u(P)$ and $\pi_1 \cap \pi_2 = \phi$. Then $F_1^{-1}(\pi_1)$ and $F_2^{-1}(\pi_2)$ are two disjoint strips on opposite sides with respect to LC_{-1}, and defining $H_1 = F_2^{-j} \circ F_1^{-1}(\pi_1)$, $H_2 = F_2^{-(j+1)}(\pi_2)$, we get two disjoint 'horizontal' strips, as close to P as we want, by fixing suitable values of the integer j. Let us assume a fixed value of j. Then $F^{j+1}(H_1 \cup H_2) = \pi_1 \cup \pi_2$ and it is easy to see that, in a finite number of iterations by F, we shall get $F^m(H_1 \cup H_2) = V_1 \cup V_2$, where V_1 and V_2 are disjoint strips which intersect $H_1 \cup H_2$ as in Fig. 14.

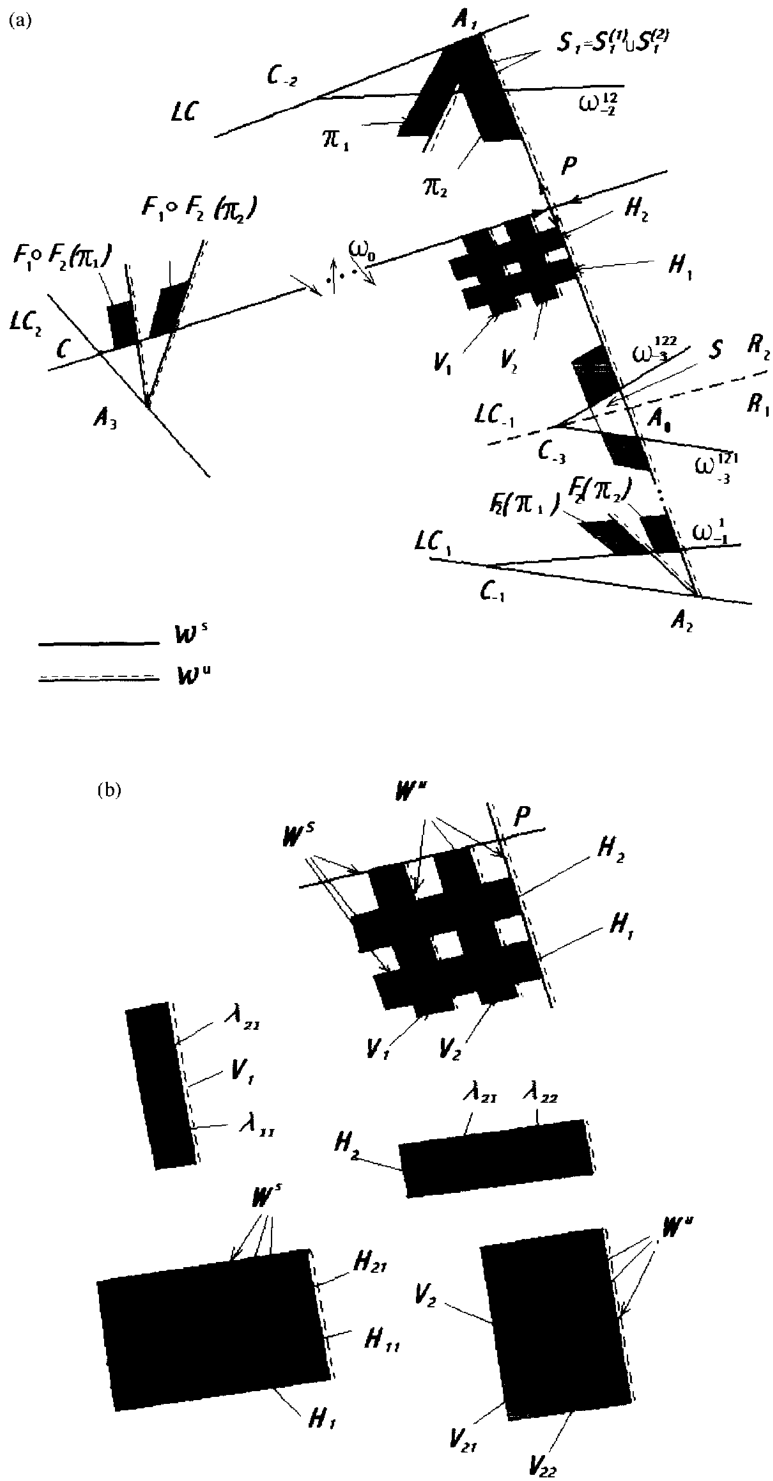

Fig. 14. Construction of Smale horseshoe (a) and its enlargements (b, c), after the first homoclinic bifurcation of saddle fixed point P (for the details see text).

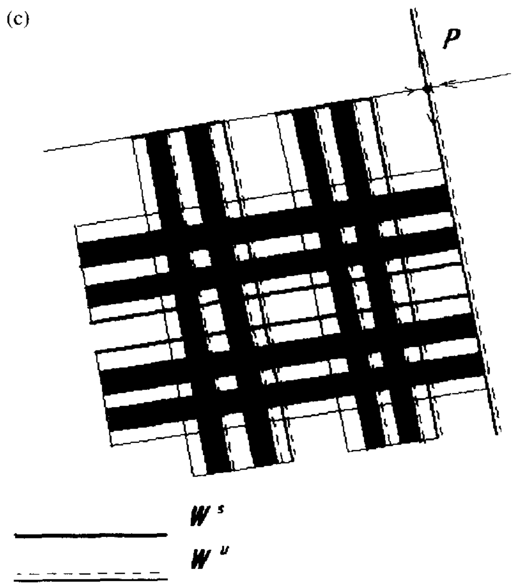

Fig. 14—*continued.*

In fact, after $(j+1)$ applications of F, we get $\pi_1 \cup \pi_2$ and then $F(\pi_1 \cup \pi_2) = F_2(\pi_1 \cup \pi_2)$, $F^2(\pi_1 \cup \pi_2) = F_1 \circ F_2(\pi_1 \cup \pi_2)$ and after i applications of $F = F_2$, for a suitable integer i, we shall be sufficiently near P to get disjoint intersections with H_1 and H_2, as in Fig. 14(a). It is now clear that the 'standard horseshoe mechanism' can be instaured, proving the existence of an invariant Cantor set, $\Lambda \subset H_1 \cup H_2$. In fact,

$$V_1 \cup V_2 = T(H_1 \cup H_2) \text{ where } T = F^m \text{ and } m = i+3+j.$$

Moreover

$$V_1 = T_1(H_1),\ V_2 = T_2(H_2)$$

where

$$T_1 = F_2^j \circ F_1 \circ F_2 \circ F_1 \circ F_2^i \quad \text{and} \quad T_2 = F_2^j \circ F_1 \circ F_2^{i+2}.$$

Thus we can consider $T{:}(H_1 \cup H_2) \to (V_1 \cup V_2)$ as a map with a unique inverse by defining T^{-1} as follows: let $x \in V_1 \cup V_2$, then $T^{-1}(x) = T_1^{-1}(x)$ if $x \in V_1$, $T^{-1}(x) = T_2^{-1}(x)$ if $x \in V_2$ where

$$T_1^{-1} = F_2^{-i} \circ F_1^{-1} \circ F_2^{-1} \circ F_1^{-1} \circ F_2^{-j} \quad \text{and} \quad T_2^{-1} = F_2^{-(i+2)} \circ F_1^{-1} \circ F_2^{-j}.$$

For the map $T{:}(H_1 \cup H_2) \to (V_1 \cup V_2)$ and its inverse T^{-1}, the standard procedure used for invertible maps works well. Let us repeat a few steps. Define $\Lambda_{ij} = H_i \cap V_j$ (see Fig. 14(b)). Consider Λ_{21} and Λ_{11} as subsets of V_1. Then they are the image by T of two subsets of H_1. Note that one side of Λ_{21} and Λ_{11}, the right one in our figure, belongs to the stable set $W^s(P)$. Thus, these sides must be the image by T of two disjoint pieces on the right side of H_1, bounded by $W^s(P)$. The opposite sides of Λ_{21} and Λ_{11} belong to the side of V_1 which is the image by T of the side of H_1 opposite to $W^s(P)$. It follows that Λ_{21} and Λ_{11} must be the image by T of two disjoint horizontal strips included in H_1, say H_{21} and H_{11}, $T(H_{11}) = \Lambda_{11}$ and $T(H_{21}) = \Lambda_{21}$, or equivalently, $T^{-1}(\Lambda_{11}) = H_{11}$ and $T^{-1}(\Lambda_{21}) = H_{21}$. Analogous reasonings lead to the definition of two disjoint strips inside H_2: $T^{-1}(\Lambda_{22}) = H_{22} \subset H_2$ and $T^{-1}(\Lambda_{12}) = H_{12} \subset H_2$, $H_{22} \cap H_{12} = \phi$.

Now, let us take the images. Consider the two subsets Λ_{21} and Λ_{22} of H_2. As these are subsets of H_2, their images by T belong to V_2. The low boundary of such subsets belong to the stable set $W^s(P)$, thus, their images by T are two disjoint pieces on the side of V_2, belonging to $W^s(P)$ (see Fig. 14(b)). The opposite sides of these subsets belong to the side of H_2 opposite to $W^s(P)$ and thus, their images by T belong to the opposite sides of V_2. That is, $T(\Lambda_{21}) = V_{21}$ and $T(\Lambda_{22}) = V_{22}$ are two disjoint 'vertical' strips belonging to V_2. In a similar way $T(\Lambda_{11}) = V_{11}$ and $T(\Lambda_{12}) = V_{12}$ are two disjoint 'vertical' strips belonging to V_1, and so on. The mechanism is standard (see e.g. [6, 7]). We shall find a Cantor set $\Lambda \subset H_1 \cup H_2$ which is both forward and backward invariant by T, i.e. $T(\Lambda) = \Lambda$ and $T^{-1}(\Lambda) = \Lambda$.

Now, regarding hyperbolicity we note that, by construction, we started with two horizontal strips H_1 and H_2, having one side on $W^s(P)$ and one side on $W^u(P)$. However, from the process of construction of the subsets H_{ij} and V_{ij} (which also have one side on $W^s(P)$ and one side on $W^u(P)$), we can deduce that, really, in a neighbourhood of P, the structure of the stable and unstable sets of P is such that $W^s(P)$ includes infinitely many 'segments parallel' to ω_0 (i.e. the local stable set $W^s_{loc}(P)$) and the same holds for $W^u(P)$: it includes infinitely many 'segments parallel' to $W^u_{loc}(P)$ (see Fig. 14(c)). Thus, we can presume to start the process with two horizontal strips, H_1 and H_2, having two opposite sides on $W^s(P)$ and the other two opposite sides on $W^u(P)$. Then the Cantor set Λ is hyperbolic.

REFERENCES

1. Fournier-Prunaret, D., Mira, C. and Gardini, L. Some contact bifurcations in two-dimensional examples. In *Proceedings ECIT '94*. World Scientific (in press).
2. Mira, C., Gardini, L., Barugola, A. and Cathala, J. C. *Chaotic Dynamics in Two-Dimensional Noninvertible Maps*. World-Scientific, Singapore., 1996.
3. Abraham, R., Gardini, L. and Mira, C., *Chaos in Discrete Dynamical Systems (A Visual Introduction in two Dimensions)*. Telos, Springer., 1997.
4. Mira, C., Rauzy, C., Maistrenko, Y., Sushko, I., Some properties of a two-dimensional piecewise-linear noninvertible map. *Int. J. Bifurcation & Chaos*, 1996, **6(12A)**, 2299–2319.
5. Gumowski, I. and Mira, C., *Dynamique Chaotique*. Cepadues Editions, Toulouse, 1980.
6. Wiggins, S. *Global Bifurcations and Chaos*. Springer-Verlag, N.Y., 1988.
7. Wiggins, S. *Introduction to Applied Nonlinear Dynamical Systems and Chaos*. Springer-Verlag, N.Y., 1990.
8. Maistrenko, Yu. L. and Sushko, I. M., Bifurcation phenomena for two-dimensional piecewise linear maps. *J. Tech. Phys.*, 1996, **37**, 371–378.